Journal of Thermal Analysis and Calorimetry, Vol. 90 (2007) 1, 167–172

THERMAL BEHAVIOR OF A BENTONITE

M. Önal and Y. Sarıkaya*

Ankara University, Faculty of Science, Department of Chemistry, Tando ğan, 06100 Ankara, Turkey

The mineralogical composition of the Kütahya calcium bentonite (CaB) from Turkey was obtained as mass% of 60% calcium rich smectite (CaS), 30% opal-CT (OCT), trace amount illite (I), and some non-clay impurities by using chemical analysis (CA), X-ray diffraction (XRD), and thermal analysis (TG-DTA) data. The crystallinity, porosity, and surface area of the samples heated between 25–1300°C for 2 h were examined by using XRD, TG, DTA and N_2-adsorption–desorption data. The position of the 001 reflection which is the most characteristic for CaS does not affect from heating between 25–600°C and then disappeared. The decrease in relative intensity (I/I_0) from 1.0 to zero and the increase in full width at half-maximum peak height (FWHM) from 0.25 to 1.0° of the 001 reflection show that the crystallinity of the CaS decreased continuously by rising the heating temperature from 25 to 900°C and then collapsed. The most characteristic 101 reflection for opals intensifies greatly between 900 and 1100°C with the opal becoming more crystalline.

The total water content of the natural bentonite after dried at 25, 105 and 150°C for 48 h were determined as 8.8, 5.0 and 2.5%, respectively. The mass loss occurs between 25 and 400°C over two steps with the maximum rate at 80 and 150°C, respectively. The exact distinction of the dehydration temperatures for the adsorbed water and interlayer water is seen almost impossible. The temperature interval, maximum rate temperature, and mass loss during dehydroxylation are 400–800°C, 670°C and 4.6–5.0%, respectively. The maximum rate temperatures for decrystallization and recrystallization are 980 and 1030°C, respectively. The changes in specific micropore volume (V_{mi}), specific mesopore volume (V_{me}), specific surface area (S) were discussed according to the dehydration and dehydroxylation of the CaS. The V_{mi}, V_{me} and S reach to their maxima at around 400°C with the values of 0.045, 0.115 $cm^3\ g^{-1}$ and 90 $m^2\ g^{-1}$, respectively. The radii of mesopores for the bentonite heated at 400°C are distributed between 1–10 nm and intensified approximately at 1.5 nm.

Keywords: *bentonite, crystallinity, porosity, smectite, thermal analysis, X-ray diffraction*

Introduction

Bentonites (rocks dominated by smectite group minerals) are used extensively in the making of foundry sand, iron ore pellets, ceramic, drilling mud, barrier for water and nuclear waste, pharmaceutical, cat litter, paint, food, rubber, perfume and plastic [1–5]. Smectite group minerals include sodium montmorillonite (NaM), calcium montmorillonite (CaM), saponite, nontronite, beidellite, and hectorite. However, the most common dominant clay minerals in bentonites are NaM or CaM. Minor clay minerals commonly found in bentonites is illite (I). Feldspars, zeolites, carbonates, and silica polymorphs (quartz and opals) may be found in bentonites in different extent as nonclay minerals [6].

Smectite is a 2:1 layer clay mineral and has two silica tetrahedral (T) sheets bonded to a central alumina octahedral (O) sheet. The net negative charge of the 2:1 (TOT) layers arising from the isomorphic substitution in the octahedral sheets of Fe^{2+} and Mg^{2+} for Al^{3+} and in tetrahedral sheets of Al^{3+} for Si^{4+} is balanced by the exchangeable cations such as Na^+ and Ca^{2+} located between the layers and around the edges [7]. Basal spacing, $d(001)$, for air dried smectites changes from 1.26 to 1.54 nm depending on type and valence of the exchangeable cations. The equivalent amount of exchangeable cations in one kilogram bentonite or smectite is defined as cation exchange capacity. Furthermore, bentonites and their dominant mineral smectites can be used selective adsorbents, production of pillared clays, and organoclays, catalysts or catalysts supports, ion exchangers, decolorizing agents, etc., depending on their surface and ion exchange properties [8, 9].

Bentonite may be subjected to high temperatures when used in iron ore compaction, ceramic industry, foundry industry, powder catalysts, and preparation of pillared clays. In addition, before construction of bridges and buildings on smectitic soils, the ground below the foundations may be heat-treated up to 600°C to harden the clays in civil engineering [10–14]. Some physico-chemical properties of bentonites such as swelling, plasticity, cohesion, compressibility, strength, cation-exchange capacity, particle size, adsorptive properties, pore structure, surface area, surface acidity, and catalytic activity as well as mineralogy are greatly affected by thermal treatment [15–22]. Due to these effects, the

* Author for correspondence: onal@science.ankara.edu.tr

1388–6150/$20.00

Akadémiai Kiadó, Budapest, Hungary
Springer, Dordrecht, The Netherlands

investigation of the crystallinity and porosity of bentonites and their major clay minerals smectites by the heating temperature has a great importance. Thermal behavior of bentonites and other clays and also their organic complexes determined by thermal analysis with combination other instrumentation [23–28].

The empty spaces in a solid which are smaller than 2 nm, between 2 and 50 nm, and greater than 50 nm are called micropores, mesopores, and macropores, respectively [29]. The radius of a pore, assumed to be cylindrical, can be taken as half of the pore width. The volume of pores in one gram solid is defined as the specific pore volume (V/cm^3 g^{-1}). The area of the inner and outer walls of the pores located within and between interparticles in one gram solid is taken as specific surface area (S/m^2 g^{-1}).

Many studies are realized on the adsorptive and catalytic properties of bentonites, smectites and their products [30–34]. However, there are a few studies for the thermal effect on these properties [18, 22, 35–37]. Therefore, the aim of this study is to investigate of the thermal effect on the crystallinity and porosity of a smectite.

Experimental

A white CaB sample taken from Kütahya region, Turkey, was used in this study. The effects of the Na_2CO_3 and H_2SO_4 treatments on some physicochemical properties of this bentonite was previously investigated [38, 39]. The natural bentonite was ground to pass through a 0.074 mm (200 mesh) sieve. The bulk chemical analysis of the natural bentonite after dried 105°C for 4 h mass% is: SiO_2, 70.70; Al_2O_3, 13.55; Fe_2O_3, 0.71; TiO_2, 0.07; MgO, 1.79; CaO, 1.88; Na_2O, 0.14; K_2O, 0.98 and loss on ignition (LOI), 9.95. The CEC of the natural sample determined by methylene blue method is 0.52 mol kg^{-1}. An orthophosphoric acid digestion at 240°C for 12 min dissolved completely the bentonite [40–42].

Bentonite samples, each having 20 g, were heated in 100°C intervals from room temperature to 1300°C and were thermally treated by maintaining at each temperature for 2 h. X-ray diffraction patterns of the natural and thermally treated samples were recorded from random mounts using a Rikagu D-max 2200 Powder Diffractometer with a Ni filter CuK_α radiation.

The differential thermal analysis (DTA) and thermogravimetry (TG) curves of the CaB samples after heating 25, 105 and 150°C were determined by an instrument (Netzsch, Model 429) at a heating rate of 10 K min^{-1}. α-Al_2O_3 was used as an inert material. Two repeated TG-DTA experiments were performed for each sample. It is not seen any considerable difference between them. The adsorption and desorption isotherm of N_2, at liquid N_2 temperature, on the natural and thermally treated samples were determined by a volumetric adsorption instrument of pyrex glass connected to high vacuum [43, 44].

Results and discussion

Mineralogy of the bentonite

XRD patterns of the natural and all thermally treated bentonite samples were examined, and representative ones, are given in Fig. 1. The most characteristic XRD peaks for CaS (001), I (001) and OCT (101) are at 1.54, 1.00 and 0.405–0.410 nm in the XRD pattern as seen Fig. 1. The bentonite contains a calcium-rich smectite (CaS) as major clay mineral and less amount illite (I) as other clay mineral. The rest are a paracrystalline silica polymorph opal-CT (OCT) in amorphous opal-A (OA) matrix and other nonclay mineral impurities. The amount of the CaS, OCT and other impurities in the bentonite are estimated as 65, 30 and 5% by mass respectively, by evaluating of the chemical analysis. While the peaks for CaS and I change, the peak for OCT does not change by thermal treatment temperature before 900°C. The peak for opal intensifies greatly between 900–1100°C with the opal becoming more crystalline [41, 42]. The increasing in intensity of the opal peak may also be due to the

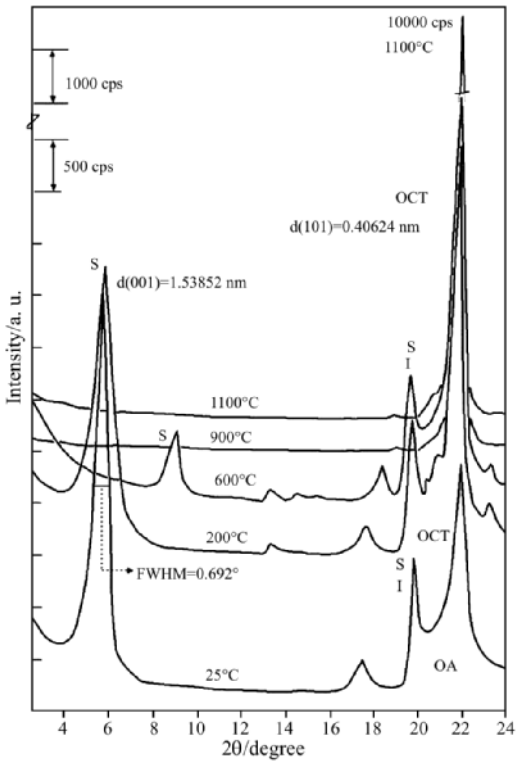

Fig. 1 X-ray diffraction patterns of the natural and some thermally treated bentonite samples at different temperatures (S – smectite, I – illite, OCT – opal-CT)

creation of new opal-like material from the decomposition of the smectite at 900°C [37].

Crystallinity change for the CaS

The position of the 001 peak shifted to right and *d*(001)-value decreased from 1.50 to 0.99 nm after heating up to 600°C, and then disappeared at 900°C, as seen in Fig. 1. The position, intensity, and full width at half-maximum peak height (FWHM) of the 001 peak for CaS change greatly by the increasing of thermal treatment temperature.

The reciprocal variations of the relative intensity (I/I_0) and FWHM of the 001 XRD peak for the CaS with the thermal treatment temperature are given in Fig. 2. Here, I_0 and I represent the intensities for the natural and heated bentonite samples, respectively. The decreasing in I/I_0 and increasing in FWHM for the 001 peak show that the crystallinity of the CaS decreases by increasing of the heating temperature.

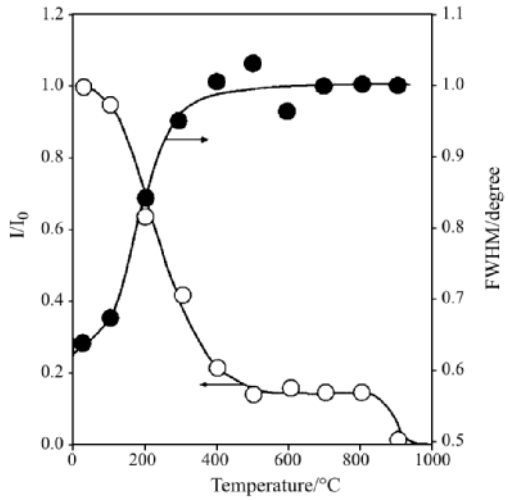

Fig. 2 The variation of the relative intensity (I/I_0) and full with at half maximum peak height (FWHM) of the 001 XRD peak for the calcium smectite (CaS) with heating temperature

Thermal analysis

Thermal analysis in combination with other techniques such as chemical and XRD analyses is suitable for the examination of minerals [45–51]. TG and DTA curves of the natural bentonite samples dried at 25, 105 and 150°C for 48 h are given in the Fig. 3 for the temperature range of 25–1100°C. Two endothermic and two exothermic changes are seen in the DTA curves. The temperature interval and maximum rate temperature of these changes are shown on the TG and DTA curves in Fig. 3.

The first and dominant endothermic mass losses of 8.8, 5.0 and 2.5% between 25 and 400°C for the

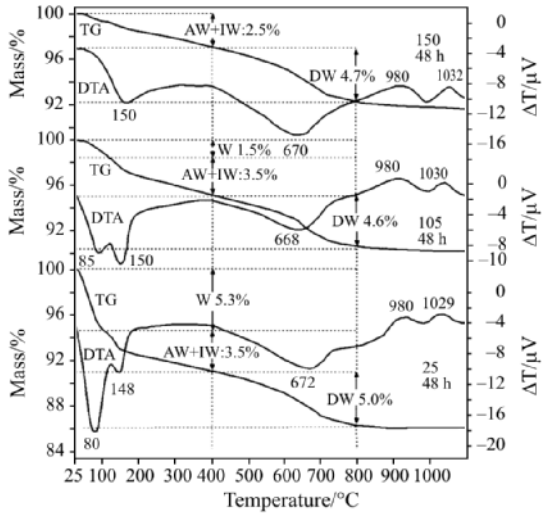

Fig. 3 Thermogravimetric analysis (TG) and differential thermal analysis (DTA) curves for the natural calcium bentonite (CaB) and its heated samples at 25, 105 and 150°C for 48 h

samples dried at 25, 105 and 150°C, respectively, are due to the dehydration of interparticle water (W), adsorbed water (AW) and interlayer water (IW). The endothermic DTA peak corresponding to these changes is twin for both samples dried at 25 and 105°C, as seen in Fig. 3. The mass losses of 5.3 and 1.5% corresponding to the first twin for the samples dried at 25 and 105°C, respectively, with the maximum rate at 80°C, are originated from dehydration of the W. This shows that the W can not be removed strictly by drying at 105°C for 48 h. The decrease in the mass of 5.3–1.5=3.8% is defined as moisture in the natural bentonite. The mass losses corresponding to the second twin with the maximum rate at around 150°C are 3.5% for the samples dried at 25°C, and 2.5% for the samples dried at 150°C. These losses are originated from the dehydration of the remained W and also AW and IW. The exactly distinguish of the dehydration temperatures for the W, AW and IW is seen almost impossible. It is concluded by combination of the thermal and XRD analyses that the AW and IW could only be removed by heating the bentonite up to 400°C.

The second endothermic mass loss of 4.6–5.0% between 400 and 800°C with the maximum rate at 668–672°C is due to the formation of dehydroxylation water (DW). The DW content does not affect from the drying temperature up to 150°C for 48 h. The first and second exothermic changes without mass loss with the maximum rates at around 980 and 1030°C are due to the decrystallization of the CaS and recrystallization of new phases, respectively. The total of the four mass losses (W+AW+IW+DW) up to 1000°C is 9.6% for the sample dried at 105°C for 48 h. This mass loss agrees well with the IOL obtained by chemical analysis as 9.95%.

Adsorption and desorption isotherms

The N_2 adsorption and desorption isotherms at the liquid N_2 temperature for all heated sample were examined and representative ones, are shown in Fig. 4. Here, p is the adsorption and desorption equilibrium pressure, p^0 is the vapor pressure of bulk nitrogen at experimental temperature, $p/p^0=x$ is the relative equilibrium pressure, and n is the adsorption capacity defined as molar quantity of nitrogen adsorbed on 1 g solid. According to Brunauer, the classification of these isotherms is similar to Type II [52, 53]. The shapes of the adsorption and desorption isotherms indicate that the bentonite is mainly a mesoporous solid but also contains some micropores. The coincidence of the adsorption and desorption isotherms over the interval $0.35<x<0$ shows that the multimolecular and monomolecular adsorption are reversible. After multimolecular adsorption up to x=0.35 was complete, capillary condensation began, and all mesopores filled up to x=0.96. Bulk liquid nitrogen forms at x=1 [54]. The liquid nitrogen outside and within the mesopores evaporates spontaneously as soon as the relative equilibrium pressure by desorption is low enough, at the interval $1<x<0.96$ and $0.96<x<0.35$, respectively. The shapes of mesopores in a solid can be cylindrical, parallel-sides silt, wedge, cavity or cone in a bottle. Capillary condensation begins from the narrowest mesopores and capillary evaporation begins from the largest mesopores. This difference almost causes the hysteresis between adsorption and desorption isotherms.

Porosity and surface area

The adsorption capacity as liquid nitrogen volume which is estimated from desorption isotherm over the interval $0.96<x<0.35$ was taken as specific micropore volume (V) for the completely full pores. The radius (r) of the largest pore full at same x was calculated from the corrected Kelvin equation corresponding to V value [29, 53]. Furthermore, V–r plots were drawn as pore size distribution (PSD) curves, and representative ones, are given in Fig. 5. The specific micro- and mesopores volume (V) and specific micropore volume were estimated from the intercepts of the extrapolation of each PSD curve to r=25 and 1 nm, respectively, according to their definitions. The specific mesopore volume (V_{me}) for each sample was taken as the difference of V–V_{mi}.

The variation of the V_{mi} and V_{me} with the heating temperature is given in Fig. 6. The V_{mi} value increases rapidly to a maximum of 0.050 $cm^3\ g^{-1}$ while the heating temperature rises to 400°C by effect of dehydration and then decreases rapidly by effect dehydroxylation and reaches to zero at 900°C by effect decrystallization. After 900°C micropores closes completely by the effect of the interparticle sintering. The V_{me} value not changes considerably up to 800°C and then decreases rapidly while the temperature increasing from 900 to 1300°C. This change is due to the collapsing of the crystal structure of the CaS and interparticle sintering. The specific surface area (S), were obtained from the standard Brunauer, Emmett and Teller (BET) method by using the adsorption data from the interval $0.05<x<0.35$ [55–58]. The variation of S with heating temperature is given in Fig. 6. The S value having initial values 42 $m^2\ g^{-1}$ increases to its maximum of 91 $m^2\ g^{-1}$ at 400°C and then decreases to zero at 1300°C almost in parallel with the V_{mi} and V_{me} values. Since the V_{mi} and S values reach maximum at 400°C, it can be purposed that the surface area is originated from

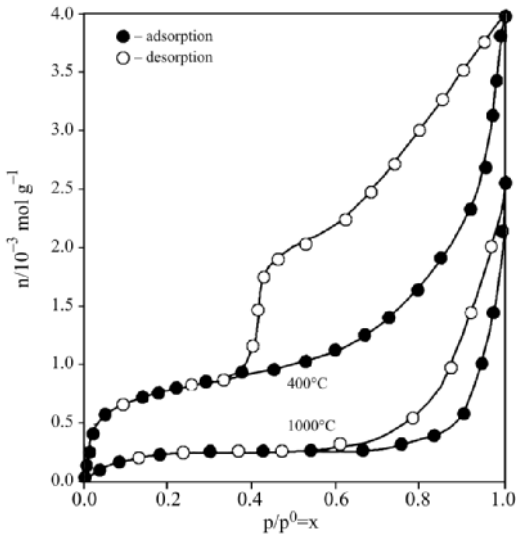

Fig. 4 The adsorption and desorption isotherms of N_2 at liquid nitrogen temperature on the heated bentonite samples at 400 and 1000°C

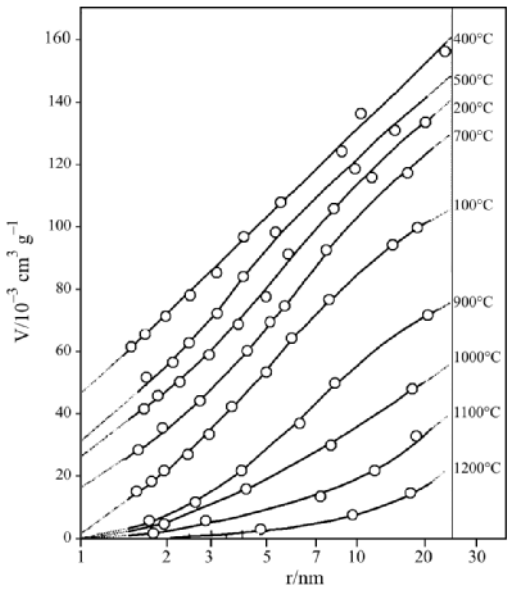

Fig. 5 The mesopore size distribution curves (V–r) for the heat treated bentonite samples

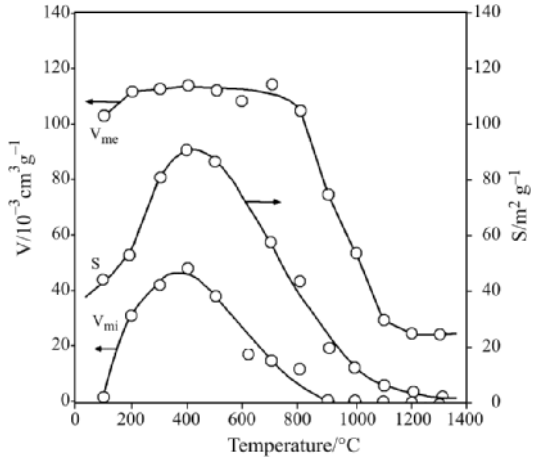

Fig. 6 The variation of specific surface area (S), specific micropore volume (V_{mi}) and specific mesopore volume (V_{me}) with the heating temperature

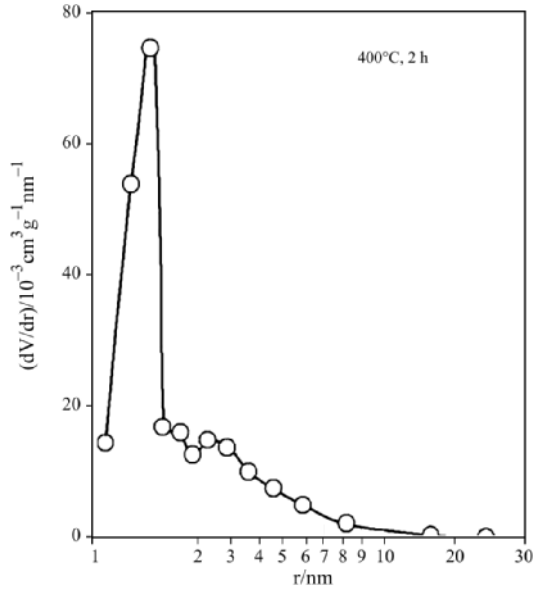

Fig. 7 The radius derivative mesopore size distribution curve (dV/dr–r) for the sample with the maximum micropore volume and surface area, obtained by heat treatment at 400°C for 2 h

the walls of micropores more than mesopores. An alternative mesopore size distribution curve (dV/dr–r) obtained as radius derivative of the V–r curve for the sample having maximum $V(V_{mi}+V_{me})$ and S values is shown in Fig. 7. As seen in this figure, the radii of mesopores are distributed between 1 and 10 nm and intensified approximately at 1.5 nm.

Conclusions

The crystallinity and porosity of smectites found in bentonites as major clay mineral reduce greatly by thermal treatment. The change by dehydration up to 400°C is reversible. Such properties after heating above 600°C reduce irreversibly. The crystal structure of the smectite collapses irreversibly at 900°C. Before construction of buildings and bridges on smectitic soils, the ground below the foundation may be heat-treated up to 600°C to harden the clay in civil engineering. The crystal structure of opal-CT found in bentonite as nonclay mineral does not affect from heat treatment up to 900°C.

Acknowledgements

The authors thank the Scientific Research Council of Ankara University for supporting this study under the project No: 2003-07.05.082.

References

1 R. E. Grim, Clay Minerology, 2nd Ed., McGraw-Hill, New York 1968.
2 R. E. Grim and N. Güven, Bentonites, Geology, Mineralogy, Properties and Uses. Development in Sedimentology, Vol. 24, Elsevier, Amsterdam 1978.
3 R. M. Barrer, Clays Clay Miner., 37 (1989) 385.
4 E. Srasra, F. Bergaya, H. van Damme and N. K. Ariquib, Appl. Clay Sci., 4 (1989) 411.
5 E. Gamiz, J. Linares and R. Delgado, Appl. Clay Sci., 6 (1992) 359.
6 D. M. Moore and R. C. Reynolds Jr., X-ray Diffraction and the Identification and Analysis of Clay Minerals, 2nd Ed., Oxford University Press, Oxford 1997.
7 H. H. Murray, Appl. Clay Sci., 17 (2000) 207.
8 T. J. Pinnavaia, Science, 220 (1983) 365.
9 R. S. Varma, Tetrahedron, 58 (2002) 1235.
10 M. C. Wang, J. M. Benway and A. M. Arayssi, In Physicochemical Aspects of Soil and Related Materials, K. B. Hoodinott, R. O. Lamb and A. J. Lutenegger, Eds, ASTM STP 1095, Philadelphia 1990, pp. 1139–1158.
11 M. M. Abu-Zreig, N. M. Al-Akhras and M. F. Attom, Appl. Clay Sci., 20 (2001) 129.
12 S. Chandrasekhar and S. Ramaswamy, Appl. Clay Sci., 21 (2002) 133.
13 Ö. Tan, L. Yılmaz and S. Zaimoğlu, Mater. Lett., 58 (2004) 1176.
14 I. Kolaríková, R. Prikryl, R. Hanus and E. Jelínek, Appl. Clay Sci., 29 (2005) 215.
15 W. F. Bradley and R. E. Grim, Am. Mineral., 36 (1951) 182.
16 G. W. Brindley, Ceramica, 24 (1978) 217.
17 T. Mozas, S. Bruque and A. Rodriquez, Clay Miner., 15 (1980) 421.
18 W. T. Reicle, J. Catal., 94 (1985) 547.
19 H. Ceylan, A. Yıldız and Y. Sarıkaya, Turk. J. Chem., 17 (1993) 267.
20 R. C. Joshi, G. Achari, D. Horfield and T. S. Nagaraj, J. Geotech. Eng. ASCE, 120 (1994) 1080.
21 M. Chorom and P. Rengasamy, Clays Clay Miner., 44 (1996) 783.

22 A. Neaman, M. Pelletier and F. Willieras, Appl. Clay Sci., 22 (2003) 153.
23 V. Balek, Z. Malék, S. Yariv and G. Matuschek, J. Therm. Anal. Cal., 56 (1999) 67.
24 E. Kristóf-Makó and A. Z. Juhász, Thermochim. Acta, 342 (1999) 105.
25 M. V. Kök and W. Smykatz-Kloss, J. Therm. Anal. Cal., 64 (2001) 1271.
26 V. Hlavatý and V. S. Fajnor, J. Therm. Anal. Cal., 67 (2002) 113.
27 M. V. Kök, Energy Sources, 24 (2002) 899.
28 M. V. Kök, Energy Sources, 26 (2004) 145.
29 S. J. Gregg and K. S. W. Sing, Adsorption, Surface Area and Porosity, 2nd Ed., Academic Press, London 1982.
30 J. M. Adams, Appl. Clay Sci., 2 (1987) 309.
31 Z. Ge, D. Li and T. J. Pinnavaia, Microporous Mater., 3 (1994) 165.
32 P. Kumar, R. V. Jasra and T. S. G. Bhat, Ind. Eng. Chem. Res., 34 (1995) 1440.
33 D. R. Brown and C. N. Rhodes, Catal. Lett., 45 (1997a) 35.
34 M. Önal, Y. Sarıkaya, T. Alemdaroğlu and İ. Bozdoğan, Turk. J. Chem., 27 (2003) 683.
35 Y. Sarıkaya, M. Önal, B. Baran and T. Alemdaroğlu, Clays Clay Miner., 48 (2000) 557.
36 T. Alemdaroğlu, G. Akkuş, M. Önal and Y. Sarıkaya, Turk. J. Chem., 27 (2003) 675.
37 H. Noyan, M. Önal and Y. Sarıkaya, Clays Clay Miner., 54 (2006) 377.
38 N. Yıldız, Y. Sarıkaya and A. Çalımlı, Appl. Clay Sci., 14 (1999) 319.
39 M. Önal, Y. Sarıkaya, T. Alemdaroğlu and İ. Bozdoğan, Turk. J. Chem., 26 (2002) 409.
40 N. A. Talvitie, Anal. Chem., 23 (1951) 623.
41 J. M. Elzea, J. E. Odom and W. J. Miles, Anal. Chim. Acta, 286 (1994) 107.
42 S. Kahraman, M. Önal, Y. Sarıkaya and İ. Bozdoğan, Anal. Chim. Acta, 552 (2005) 201.
43 Y. Sarıkaya and S. Aybar, Commun. Fac. Sci. Uni. Ank., 24B (1978) 33.
44 Y. Sarıkaya, İ. Sevinç and M. Akınç, Powder Technol., 116 (2001) 109.
45 M. Gal, J. Thermal Anal., 37 (1991) 1621.
46 A. Acosta, I. Iglesias, M. Aineto, M. Romero and J. Ma. Rincón, J. Therm. Anal. Cal., 67 (2002) 249.
47 H. Zou, M. Li, J. Shen and A. Auroux, J. Therm. Anal. Cal., 72 (2003) 209.
48 A. Fodor, L. Ghizdavu, A. Suteu and A. Caraban, J. Therm. Anal. Cal., 75 (2004) 153.
49 J. Ma. Rincón, M. Romero, A. Hidalgo and Ma. J. Liso, J. Therm. Anal. Cal., 76 (2004) 903.
50 N. Yener, M. Önal, G. Üstünışık and Y. Sarıkaya, J. Therm. Anal. Cal., OnlineFirst, DOI: 10.1007/s10973-005-7459-0.
51 H. Bayram, M. Önal, G. Üstünışık and Y. Sarıkaya, J. Therm. Anal. Cal., OnlineFirst, DOI: 10.1007/s10973-006-7561-y.
52 S. Brunauer, L. S. Deming, D. M. Deming and E. Teller, J. Am. Chem. Soc., 62 (1940) 1723.
53 F. Rouquerol, J. Rouquerol and K. Sing, Adsorption by Powder and Porous Solids, Academic Press, London 1999.
54 B. G. Linsen, Physical and Chemical Aspects of Adsorbent and Catalysts, Academic Press, London 1970.
55 S. Brunauer, P. H. Emmett and E. Teller, J. Am. Chem. Soc., 60 (1938) 308.
56 A. L. McClellan and H. F. Hornsberger, J. Colloid Interface Sci., 23 (1967) 577.
57 D. H. Everett, G. D. Parfitt, K. S. W. Sing and R. Wilson, J. Appl. Chem. Biotechnol., 24 (1974) 199.
58 A. U. Doğan, M. Doğan, M. Önal, Y. Sarıkaya, A. Aburub and D. E. Wurster, Clays Clay Miner., 54 (2006) 62.

Received: July 10, 2006
Accepted: October 3, 2006
OnlineFirst: February 13, 2007

DOI: 10.1007/s10973-005-7799-9